

Phylogenetic Relationships among the Mosses Based on Heterogeneous Bayesian Analysis of Multiple Genes from Multiple Genomic Compartments

CYMON J. COX,^{1,3} BERNARD GOFFINET,² A. JONATHAN SHAW,¹ and SANDRA B. BOLES¹

¹Department of Biology, Science Drive, Duke University, Durham, North Carolina 27708;

²Department of Ecology and Evolutionary Biology, University of Connecticut, Connecticut 06269;

³Author for correspondence (cymon@duke.edu)

Communicating Editor: Aaron Liston

ABSTRACT. Nucleotide sequences from eight nuclear, chloroplast, and mitochondrial genes were obtained from 30 mosses (plus four outgroup liverworts) in order to resolve phylogenetic relationships among the major clades of division Bryophyta. Phylogenetic analyses were conducted using maximum parsimony, maximum likelihood (ML), and Bayesian inference. Inferences were compared from Bayesian analyses using homogeneous and several heterogeneous models. Estimates of clade confidence were based on bootstrap analyses, posterior probabilities (in Bayesian analyses) and novel combined approaches. Most ingroup relationships were congruent among analyses, but support for individual clades depended on the analytical approach. Increasingly parameterized models of nucleotide substitution in the likelihood analyses provided significantly higher goodness-of-fit to the data. The results suggest that 1) the Bryophyta, including *Sphagnum* and *Takakia*, are monophyletic, 2) *Andreaea* and *Andreaebryum* form a monophyletic group, 3) *Oedipodium griffithianum* is sister to all other operculate taxa, 4) mosses with nematodontous peristomes are paraphyletic and basal to arthrodontous mosses, 5) *Diphyscium* is sister to all other arthrodontous mosses, 6) *Encalypta* is sister to the Funariaceae, and 6) mosses with diplolepidicous-alternate peristomes form a monophyletic group. Implications of the phylogenetic hypothesis for morphological evolution in mosses include 1) a pseudopodium has arisen independently in *Sphagnum* and *Andreaea*, 2) the mucilage hairs of *Andreaebryum* and *Takakia* are non-homologous, 3) the stomata found in *Sphagnum* are not homologous to those of other mosses, and 4) that stomata were absent in the ancestor of all mosses.

The mosses (Bryophyta) are represented on all continents and form a conspicuous element of the vegetation in many environments. Comprising approximately 12,500 species (Crosby et al. 1999), the mosses are also the most speciose non-vascular plant group. The gametophyte forms the vegetative and dominant stage of the life-cycle, while the sporophyte is unbranched, ephemeral, and completes its full development attached to the maternal gametophyte. The mosses are distinguished from other non-vascular plants, namely the liverworts (Marchantiophyta) and hornworts (Anthoceroophyta), by a number of developmental and morphological characters. Moss sporophytes are more anatomically complex than are those of liverworts and hornworts, and the seta develops fully before differentiation of the capsule (sporangium). Mosses typically have hygroscopic peristome teeth surrounding the mouth of the operculate capsule whereas liverwort and hornwort capsules lack opercula and peristomes. The gametophytes of leafy liverworts look superficially similar to those of mosses, but differ in complexity and anatomical detail. The mosses, either alone or in a clade with the liverworts, form the sister group to the tracheophytes (e.g., Lewis et al. 1997; Hedderon et al. 1998; Nickrent et al. 2000); *ipso facto*, they form a pivotal group for understanding the evolutionary transition of plants to a terrestrial habitat and the evolutionary trajectory of developmental processes and life-history traits leading to the tracheophytes (Garbary et al. 1993; Goffinet 2000; Newton et al. 2000; Renzaglia et al. 2000).

Traditional classifications of the mosses have usually emphasized either the gametophyte (e.g., Schimper 1853–55; Kindberg 1897) or the sporophyte (e.g., Palisot de Beauvois 1805; Mitten 1859) as the primary source of characters defining major groups. The division of the mosses into ‘acrocarpus’ and ‘pleurocarpus’ is based on the position of the archegonia (and hence the sporophyte) with respect to the stem apex. Throughout much of the nineteenth century, this gametophytic distinction formed the basis for the primary taxonomic division of the mosses. In contrast, for most of the twentieth century, beginning with the seminal flora of Fleischer (1904–23), followed by Brotherus (1924–25), higher-level taxonomic groups have been largely characterized by features associated with the peristome teeth of the sporophytic capsule, with only secondary consideration given to characters of gametophytic architecture. Observations on peristome architecture from which these classifications derived were made by Philibert (1884–1902), and became such a pervasive *modus operandi* that the Brotherus-Fleischer system remained largely intact (Vitt 1984) until cladistic and molecular phylogenetic methods were applied to moss systematics. Typical justification given for the emphasis on peristome characters was their supposed evolutionary stability, presumed to reflect relatively weak selective pressures on the temporally-transient sporophyte (e.g., Buck and Crum 1978; Buck 1980).

Two general forms of the moss peristome are recognized: nematodontous peristomes consist of teeth

made of whole, elongated, dead cells (characteristic of the orders Polytrichales and Tetraphidales), whereas arthrodontous peristomes consist of articulated teeth composed of the remnants of cell walls. Both peristome types exhibit variation in number, fusion, and orientation of teeth, and may be developmentally reduced, or even absent. Arthrodontous peristomes are further categorized as haplolepeidous (e.g., in the Dicranales and Grimmiiales), in which the outer surface of each tooth consists of a single vertical row of cell plates, and diplolepeidous, in which there are two vertical rows of plates per tooth (e.g., in the Bryales and Funariales). Furthermore, diplolepeidous peristomes are typically composed of two rows of teeth, with the inner row (i.e., the endostome) homologous in position and development to the single row of teeth typically exhibited by the haplolepeidous peristome. The outer row (i.e., exostome) of haplolepeidous peristomes is usually absent or very reduced. Two types of diplolepeidous peristome are distinguished based on the position of the endostome teeth, or segments, relative to the exostome teeth. The diplolepeidous-opposite peristome, exemplified by *Funaria* Hedw. (Funariales), has endostome segments lying opposite the exostome teeth, while the diplolepeidous-alternate peristome, exemplified by *Bryum* Hedw. (Bryales), has endostome segments alternating radially with the exostome teeth. The *Bryum*-type is further characterized by the presence of cilia, narrow appendages formed between the segments, and hence opposite the exostome teeth. The Orthotrichaceae (Orthotrichales) have alternate peristomes but lack cilia, a combination that prompted Vitt (1981) to recognize a fourth architectural type of arthrodontous peristome, the Orthotrichum-type peristome (but see Shaw 1986; Goffinet et al. 1999).

Despite the generality of these peristome types, some groups of mosses do not fall neatly into the categories. The Buxbaumiinae sensu Vitt comprise two families, the Buxbaumiaceae and the Diphysciaceae, characterized by reduced gametophytes and massive, asymmetric sporophytes. These families differ in their peristomial architecture, but neither fits any of the above types. In fact the peristome of *Buxbaumia* is composed of several rows of teeth and combines nematodontous and arthrodontous elements. That of *Diphyscium* is composed of two rows only, but the inner teeth are fused into a pleated membrane. Vitt (1984) considered this peristome to be most similar to that of the Encalyptaceae. Developmental studies (Shaw et al. 1987, 1989a, b; Shaw and Anderson 1988; Goffinet et al. 1999) have shown that all types share a fundamental pattern of early development with the main distinction lying in the symmetry of the second anticlinal division in the inner peristomial layer (IPL). This division is asymmetric in the Haplolepeidae, the Bryales sensu lato, *Diphyscium* and *Tetraphis*, and symmetric in

the Funariaceae, and the Polytrichaceae (Goffinet et al. 1999). In summary, peristome types are defined by whole versus partial cells, opposite versus alternate arrangement of teeth, the architecture of the endostome, and the mode of cell division in the IPL. While these characters seem to be useful for defining major groups of mosses, they are insufficient for resolution of phylogenetic relationships among lineages (Vitt et al. 1998; Goffinet et al. 2001). A robust independently derived phylogenetic hypothesis is needed for reconstructing the evolution of mosses and transformations in peristome architecture.

A number of different methodologies have previously been used to reconstruct phylogenetic relationships among major groups of mosses (e.g., Hedderson et al. 1996, 1998; Beckert et al. 1999, 2001; Cox and Hedderson 1999; Newton et al. 2000; Goffinet et al. 2001). These studies differed with regard to breadth of taxonomic sampling, the quantity and variety of data, and the reconstruction methods employed, but agreed on many of their conclusions. The nematodontous mosses are often found to be paraphyletic and basal to the arthrodontous mosses. The arthrodonts themselves form a monophyletic group in which the diplolepeidous mosses are basal-most and paraphyletic with respect to a monophyletic clade of haplolepeidous mosses. The two pleurocarpous orders (i.e., Hookeriiales and Hypnales) form a monophyletic group derived from a grade of acrocarpous families.

The earliest diverging lineages of the mosses are less clearly established; few studies have possessed sufficient taxonomic sampling to address placement of the root-node of the mosses. Of particular importance with respect to the root-node is the placement of *Sphagnum* and *Takakia*. The studies of Hedderson et al. (1998) and Newton et al. (2000) both resolved (with weak support) *Sphagnum* and *Takakia* as sister taxa, albeit in the Newton et al. study the clade was sister to all mosses, whereas in the Hedderson et al. study the clade was sister to the arthrodontous mosses. In addition, the study of Yatsentyuk (2001) placed *Takakia* alone as the sister taxon to all other mosses.

The aim of the analyses presented here is to resolve relationships among the major lineages of mosses and assess the statistical support for those relationships with respect to molecular markers from all three genomic compartments. Specifically, we address the question of the monophyly of mosses, the placement of the root-node, the affinities of *Sphagnum* and *Takakia*, and the topology of acrocarpous lineages leading to the pleurocarpous mosses.

Modeling Heterogeneous Data. The application of Bayesian statistics in phylogenetics (for review see Lewis 2001) has greatly reduced the computational burden of maximum likelihood based analyses, although the interpretation of Bayesian posterior prob-

abilities in relation to more usual statistical measures of confidence (i.e., the non-parametric bootstrap) is not straight-forward (Huelsenbeck et al. 2002; Susuki et al. 2002; Alfaro et al. 2003). The juxtaposition of non-parametric bootstrap support values and Bayesian posterior probabilities stems from their differing statistical paradigms (Shoemaker et al. 1999). The non-parametric bootstrap (Felsenstein 1985) is based on classical frequentist statistics that typically involve the construction of confidence intervals, whereas Bayesian statistics focus on a direct assessment of probability of a hypothesis conditional on the data. The latter perspective is preferred because it directly focuses on the probability for the hypothesis in question rather than on the likelihood of the data given the hypothesis (Lewis 2001). In a phylogenetic context, Alfaro et al. (2003) suggest that the bootstrap be interpreted as a measure of 'repeatability'; that is, the sensitivity of the results to sampling error associated with drawing characters from a hypothesized underlying character distribution. In this sense, the bootstrap provides a valuable and complementary measure of confidence to a direct Bayesian probability for the results conditioned on the data and model. The non-parametric bootstrap is especially valuable as Bayesian phylogenetic analysis has been shown in simulation to be more susceptible to assigning high confidence to incorrect short branches than is the bootstrap, leading to excessive type-1 error rate rates (Susuki et al. 2002; Alfaro et al. 2003).

The analysis of multiple loci under the parsimony criterion necessarily implies a single molecular evolutionary model common to all data partitions, and while it is theoretically possible to implement multiple models simultaneously under the maximum likelihood criterion, these analyses are typically impractical given the large computational time required. Consequently, it is often necessary that a model-based ML analysis be conducted with a single substitution model applied to all data partitions with little consideration of the goodness-of-fit of the model to the data, even though, *a priori*, one would expect individual loci to be evolving under different constraints and hence substitution models. In addition to standard phylogenetic methods (i.e., parsimony and maximum likelihood) we employ heterogeneous Bayesian phylogenetic analyses implemented in P4 (Foster 2002) and MrBayes3 (Huelsenbeck and Ronquist 2002) that enable the modeling of data partitions (and sub-partitions) individually within the context of a simultaneous analysis. Several nested models of increasing complexity are employed to assess the effect of model accuracy on the Bayesian results. To offset the excessive type-1 error rates associated with Bayesian posterior probabilities, we also implement a Bayesian bootstrapping technique to assess the repeatability of the Bayesian analyses.

MATERIALS AND METHODS

Taxon and Gene Sampling. Thirty taxa were sampled from all orders of mosses (Table 1) currently recognized on the basis of previous molecular analyses (see Buck and Goffinet 2000). Four liverwort taxa were included as outgroups. Taxa and GenBank accession numbers for sequences used in the analyses are given in the Appendix. Species identifications were confirmed by the authors. Eight DNA regions were selected for analysis: the nuclear 18S ribosomal RNA (nuc18S) and partial 26S ribosomal RNA (nuc26S) gene sequences, mitochondrial intron sequences from NADH protein-coding subunits 5 & 7 (*nad5* and *nad7*), chloroplast ribosomal small protein 4 (*rps4*) gene, the *trnL* (UAA) 5' exon—*trnF* (GAA) region (*trnL*), the photosystem II 32K protein (*psbA*) protein gene, and the ribulose bis-phosphate carboxylase (*rbcL*) gene. The data matrix and trees can be found in TreeBASE (study accession number S940, matrix accession number M1558).

DNA Extraction and Amplification. Total genomic DNA was extracted using the method of Edwards et al. (1991), or a standard CTAB procedure (Doyle and Doyle 1987), with subsequent cleaning using the Wizard DNA Clean-up Kit (Promega) and elution in 50 µL of water. Double-stranded DNA templates were prepared by polymerase chain reaction (PCR), employing 30 cycles of 1 min. at 97°C, 1 min. at 52°C and 3 min. at 72°C, preceded by an initial melting step at 97°C, and followed by a final extension period of 7 min. at 72°C. The annealing temperature was lowered to 45°C when amplification failed at the higher temperature. Amplification and sequencing primers follow Cox et al. (2000) for the nuc18S, *rbcL*, *rps4*, and *trnL* DNA regions. The following regions were amplified and sequenced using novel primers (unless stated otherwise): *Nad5*—*nad5-F4* (GAAGGAGTAGGTCTCGTTCA -forward), *nad5-R3* (AAAACGCCTGCTGTACCAT—reverse), and *Ki* (ACT YGG TTA CY GAT GCA ATG GAG GGT—forward) (Beckert et al. 1999) for sequencing only; *nad7*—*nad7-F3* (ATCTCGGCA-CAGCGGAAC—forward), *nad7-R3* (CGCTGGCATCTCTCATTCA—reverse), and *nad5-R1* (CCTCCCTGGCTTGACCTT—reverse) for sequencing only; *nuc26S*—*LS0F* (ACCCGCTGTTAAGCATAT—forward), *LS12R* (ATCGCCAGTTCGTTACCA—reverse), and *LS4F* (AGGACTTTAAAAGAGAGTC—forward) (P. Manos, pers. comm.) for sequencing only; *psbA*—*trnK2F* (GACGAGTTCCGGGTTTCGA—forward), *psbA576R* (TGGAATGGGTGCA-TAAGG—reverse), *psbA501F* (TTTCTCAGACGGTATGCC—forward), and *trnHR* (GAACGACGGGAATTGAAC—reverse). Amplification was achieved using 2.5 units *Taq* polymerase (Perkin Elmer) in a 100 µL reaction volume (1x thermostable buffer, 2.5mM MgCl₂, 200mM dNTPs, 300mM primer). Fragments were cleaned on a QIAquick (Qiagen) PCR purification spin column and sequenced using each amplification primer in conjunction with the ABI Prism Dye Terminator Cycle Sequencing Ready Reaction Kit (P. E. Applied Biosystems). Sequencing products were resolved on an ABI (model 3700) automated sequencing machine.

Sequence Editing and Alignment. For each taxon and sequenced DNA region, forward (5'-3') and reverse (3'-5') sequences were assembled and checked for inaccurate base calling using Sequencher (vers. 4.1, Gene Codes Corp.). Consensus sequences were aligned manually using Se-AL (vers. 2, <http://evolve.zoo.ox.ac.uk/software/Se-AL/main.html>) and regions of ambiguous alignment and incomplete data (i.e., at the beginning and end of sequences) were identified and excluded from subsequent analyses.

Phylogenetic Analyses. Phylogenetic analyses employing maximum parsimony and likelihood optimality criteria were conducted using PAUP4.0b8-10 (Swofford 2002) mounted on an AMD Athlon-based Red Hat Linux 2.4.17-0.13 and seven Intel-based Red Hat Linux 2.4.18-10 PC's. Bayesian inference procedures were performed using MrBayes2 (Huelsenbeck and Ronquist 2001), MrBayes3 (Huelsenbeck and Ronquist 2002), and P4 (Foster 2002), on the same computing architecture.

MAXIMUM PARSIMONY ANALYSES. Non-parametric bootstrap analyses under parsimony were conducted (after deletion of parsimony uninformative characters) for each data partition (DNA region) using 300 replicates, each with two random-taxon addition replicates with tree bisection and reconnection (TBR) branch-

TABLE 1. Taxa sampled in this study. Moss classification follows Buck and Goffinet 2000. Liverwort classification follows Crandall-Stotler and Stotler 2000. Herbaria: DUKE—Duke University, U.S.A.; RNG—The Reading University, U.K. N/A: no additional sequences obtained for this study.

Taxon	Order	Family	Voucher
Outgroup Taxa			
<i>Haplomitium hookeri</i> (Sm.) Nees	Haplomitriales	Haplomitriaceae	<i>Schofield</i> 95224 (DUKE)
<i>Pellia epiphylla</i> (L.) Corda	Fossombroniales	Pelliaceae	<i>Risk & Gross</i> 12231 (DUKE)
<i>Porella pinnata</i> L.	Porellales	Porellaceae	<i>Goffinet</i> 4744 (DUKE)
<i>Preissia quadrata</i> (Scop.) Nees	Marchantiales	Marchantiaceae	<i>Schofield</i> 105579 (DUKE)
Ingroup Taxa			
<i>Alphosia azoricum</i> (Ren. & Card.) Card.	Polytrichales	Polytrichaceae	<i>Rumsey, s.n.</i> (DUKE)
<i>Andreaea wilsonii</i> Hook. f.	Andreaeales	Andreaeaceae	<i>Schofield</i> 110817 (DUKE)
<i>Andreaebryum macrosporum</i> Steere & B. M. Murray	Andreaebryales	Andreaebryaceae	<i>Schofield</i> 78094 (DUKE)
<i>Aulacomnium turgidum</i> (Wahlenb.) Schwägr.	Bryales	Aulacomniaceae	<i>Hedderson</i> 6385 (RNG)
<i>Bartramia stricta</i> Brid.	Bryales	Bartramiaceae	<i>Longton</i> 4871 (RNG)
<i>Brachythecium salebrosum</i> (Hoffm. ex F. Weber & D. Mohr) Schimp.	Hypnales	Brachytheciaceae	<i>Goffinet</i> 4723 (DUKE)
<i>Buxbaumia aphylla</i> Hedw.	Tetraphidales	Buxbaumiaceae	<i>Belland</i> 16889 (DUKE)
<i>Dendroligotrichum dendroides</i> (Brid. ex Hedw.) Broth.	Polytrichales	Polytrichaceae	<i>Goffinet</i> 5425 (DUKE)
<i>Diphyscium foliosum</i> (Hedw.) D. Mohr	Diphysciales	Diphysciaceae	<i>Goffinet</i> 4492 (DUKE)
<i>Encalypta ciliata</i> Hedw.	Encalyptales	Encalyptaceae	<i>Schofield</i> 98872 (DUKE)
<i>Entosthodon laevis</i> (Mitt.) Fife	Funariales	Funariaceae	<i>Goffinet</i> 5601 (DUKE)
<i>Fissidens subbasilaris</i> Hedw.	Dicranales	Fissidentaceae	<i>Goffinet</i> 5263 (DUKE)
<i>Funaria hygrometrica</i> Hedw.	Funariales	Funariaceae	<i>Cox</i> 148 (RNG)
<i>Hedwigia ciliata</i> (Hedw.) P. Beauv.	Hedwigiales	Hedwigiaceae	<i>Hedderson</i> 11771 (RNG)
<i>Hookeria lucens</i> (Hedw.) Sm.	Hookeriales	Hookeriaceae	<i>Cox</i> 118 (RNG)
<i>Mielichhoferia elongata</i> (Hoppe & Hornsh.) Nees & Hornsch.	Bryales	Mniaceae	<i>Shaw s.n.</i> (RNG)
<i>Oedipodium griffithianum</i> (Dicks.) Schwägr.	Tetraphidales	Oedipodiaceae	<i>Schofield</i> 98670 (DUKE)
<i>Orthodontium lineare</i> Schwägr.	Bryales	Orthodontaceae	<i>Hedderson s.n.</i> (RNG)
<i>Orthotrichum hüllii</i> Hook. & Taylor	Orthotrichales	Orthotrichaceae	<i>Hedderson</i> 5745 (RNG)
<i>Polytrichadelphus purpureus</i> Mitt.	Polytrichales	Polytrichaceae	<i>Cox</i> 84/01 (DUKE)
<i>Polytrichum pallidisetum</i> Funck	Polytrichales	Polytrichaceae	<i>Goffinet</i> 4581 (DUKE)
<i>Pyrrhobryum vallis-gratiae</i> (Hampe ex Müll. Hal.) Manuel	Rhizogoniales	Rhizogoniaceae	<i>Hedderson</i> 11755 (RNG)
<i>Rhodobryum giganteum</i> (Schwägr.) Paris	Bryales	Bryaceae	<i>Longton</i> 5073 (RNG)
<i>Scouleria aquatica</i> Hook.	Grimmiales	Scouleriaceae	<i>Hedderson</i> 5811 (RNG)
<i>Sphagnum palustre</i> L.	Sphagnales	Sphagnaceae	<i>Schofield</i> 80563 (DUKE)
<i>Takakia lepidiozioides</i> S. Hatt. & Inoue	Takakiales	Takakiaceae	<i>Schofield</i> 86563 (DUKE)
<i>Tetraphis pellucida</i> Hedw.	Tetraphidales	Tetraphidaceae	N/A
<i>Tetraplodon mnioides</i> (Sw. ex Hedw.) Bruch & Schimp.	Splachnales	Splachnaceae	<i>Söderström s.n.</i> (RNG)
<i>Timmia megapolitana</i> Hedw.	Timmiales	Timmiaceae	<i>Schofield</i> 97597 (DUKE)

swapping, and saving no more than 20 trees per replicate. Taxonomic congruence among data partitions was investigated by visually inspecting bootstrap consensus trees for conflicting nodes supported at greater than 70% (Hillis and Bull 1993).

A heuristic search procedure with 1,000 random taxon-addition replicates was performed using the parsimony criterion with all data partitions included and all characters equally-weighted to identify the most-parsimonious trees. Support for nodes under parsimony was assessed by 300 non-parametric bootstrap replicates each with two random-taxon addition replicates and TBR branch-swapping.

The effects of unidentified multiple-hits and potential substitutional saturation at first, second, and third codon positions of *rps4*, *rbcL*, and *psbA* were assessed by plotting uncorrected P-distances versus F84 corrected distances, the latter incorporating unequal base frequencies and separate transition and transversion rates (Felsenstein 1984). Pairwise distances for each taxon pair under the two models were plotted using the GnuPlot graphing program (Williams and Kelley 1998). A transversion matrix was constructed from all third positions of the three coding genes by recoding

A+G as R and T+C as Y, and this matrix was combined with the original nucleotide matrix. A heuristic search and non-parametric bootstrap under the parsimony criterion were conducted, as described above, on the new combined matrix with the 3rd positions of the three coding gene replaced by the transversion matrix.

MAXIMUM LIKELIHOOD AND BAYESIAN ANALYSES. For the entire dataset, and for each gene/region partition, a homogeneous model was assigned as determined by a hierarchical likelihood ratio test among 24 models conducted with the aid of Mr-Modeltest-1.1b (Nylander 2002). The single maximum parsimony tree was used as the object tree for calculation of the likelihoods during analyses of the models.

The optimal model for the entire dataset, namely the general time-reversible model (GTR+I+G—Rodriguez et al. 1990) with a proportion of invariable characters and other site rates modeled by a discrete gamma distribution, and its estimated parameters (Table 3), were fixed in likelihood analyses. Optimal trees under the maximum likelihood criterion were sought using 100 replicates of random taxon-addition to the starting tree. Support for nodes under ML was assessed by 100 non-parametric bootstrap repli-

cates, with each replicate consisting of a single heuristic search starting from a random taxon-addition tree with TBR branch-swapping.

Bayesian phylogenetic analyses were performed using MrBayes2 with a homogeneous model (as previously calculated) across all eight partitions with two runs, each with 200,000 generations, and four runs, each with 2,000,000 generation, using default, uniform priors. Model parameters including trees were sampled every 100th generation under a general time-reversible (GTR) model of DNA substitution with ML-estimated base composition and among-site rate heterogeneity modeled by a gamma distribution with an estimated shape parameter. The number of trees needed to reach stationarity (i.e., the “burn-in”) in the MCMC algorithm was estimated by visual inspection of the plot of ML score at each sampling point using GnuPlot. The trees of the burn-in for each run were excluded from the tree set, and the trees from each run combined to form the full sample of trees assumed to be representative of the posterior probability (p.p.) distribution.

Heterogeneous Bayesian analysis was performed using P4 with a separate sub-model for each of the eight partitions (8-part analysis), with sub-model definitions for each partition assigned to the selected models as determined by MrModeltest as described above. Heterogeneous models are referred to in this text by their number of modeled partitions (sub-models), though clearly the model applied to the data is a combination of the sub-models for each partition. The analyses were repeated with the same eight sub-models plus an additional parameter (RR) for the relative substitution rate of each partition (8-part-RR analysis). In addition a heterogeneous Bayesian analysis was performed with sub-models for each partition plus a separate sub-model for each protein-coding gene at the 3rd positions (12-part analysis) and a further sub-model for the non-coding region of the *psbA* sequences. The 12-part analyses were repeated with the addition of the relative rate parameter (12-part-RR analysis). Sub-models appropriate to the first- plus second-positions, and the third-positions of each protein-coding gene (*rps4*, *rbcL*, and *psbA*), and the non-coding region of *psbA* were assessed using MrModeltest. During each analysis, parameters of the model were estimated during the MCMC chain. Each chain was run for 100,000 generations sampling every 10th generation, and repeated five times using the optimal homogeneous ML tree as the starting tree but with a different random number seed. All analyses used default (flat) priors, and parameter acceptance rates for each analysis were tuned to between 15–30%. The assessment of the burn-in and calculation of the posterior probabilities were as described above.

BAYESIAN BOOTSTRAP ANALYSES. Non-parametric bootstrap analyses of the 8-part and 12-part datasets were performed under a heterogeneous Bayesian methodology. For both datasets, each of the data partitions (8 and 12, respectively) was individually bootstrapped and combined to form the replicate data matrix using a custom-made extension method of P4. For both datasets 100 bootstrap matrices were constructed. Each bootstrap matrix was analyzed using MrBayes3 with two MCMC runs each of 100,000 generations for the 8-part datasets and 200,000 generations for the 12-part datasets, sampling at every 100th generation. Sub-model definitions (applying to the individual partitions) were determined by MrModeltest (as described above) with parameter values estimated during the MCMC chain. Each sub-replicate was plotted in GnuPlot to determine the burn-in and compared for convergence with the other sub-replicates.

After deletion of the burn-in tree-set, trees from the posterior distribution of each sub-replicate were combined to form the union-set of each replicate using PAUP. For each replicate, the ‘sumt’ command of MrBayes3 was applied, and the tree-set of all trees within the 95% cumulative probability of the posterior distribution determined. A 50% majority-rule consensus tree was calculated in PAUP of all trees within the 95% cumulative probability of the posterior distribution in each of the 100 replicate union-sets, weighted by the posterior probability of the individual trees.

RESULTS

DNA Sequence Characteristics. Mitochondrial sequences for outgroup taxa were unobtainable, as were

the following ingroup sequences: *nad5*—*Andreaeobryum*, *Tetraplodon*; *nad7*—*Andreaeobryum*, *Buxbaumia*, *Mielichhoferia*, *Mnium*, *Rhodobryum*. Nuclear 18S sequences were missing for *Alophosia*, as were nuclear 26S for *Polytrichum* and *Tetraplodon*. Chloroplast *trnL-trnF* sequences were missing for *Alophosia*, *Andreaeobryum*, and *Pellia*, and *psbA* was missing for *Tetraphis*. Alignment of the combined DNA sequence data resulted in a total of 11,071 aligned sites: 1895 nuc18S sites, 1207 nuc26S sites, 2089 *nad5* sites, 985 *nad7* sites, 612 *rps4* sites, 954 *trnL-trnF* sites, 1732 *psbA* sites, and 1597 *rbcL* sites. A total of 3403 sites were excluded due to missing data at the beginning or end of sequences, or ambiguous alignment across taxa, leaving 7668 sites included in the combined matrix. Of the included sites, 2369 sites were variable and 1388 parsimony informative.

Of the protein-coding genes, *rps4* included 67 first-, 47 second-, and 122 third-position parsimony informative characters, *psbA* included 23 first-, 7 second-, and 187 third-position parsimony informative characters, and *rbcL* included 54 first-, 23 second-, and 277 third-position parsimony informative characters. Plots of uncorrected P-distance versus F84 distances for transitions and transversions at third-positions of the three genes are shown in Fig. 1. The large departure from the diagonal in third-position transitions in the three genes indicates substantial unaccounted genetic distance at these sites in the uncorrected distances, suggesting high substitutional turn-over (multiple-hits) and possible saturation at these positions for transitions (Fig. 1b, d, f). In contrast, transversions at these sites (Fig. 1a, c, e), and both transition and transversions at other codon positions (data not shown), indicate less discordance between the two genetic distances and a lesser effect of multiple substitutions at these sites.

Maximum Parsimony Analyses. Separate non-parametric bootstrap analyses of each gene/region resulted in bootstrap trees for *nad5*, *nad7*, nuc26s, *rps4*, and *rbcL* that did not conflict with regard to nodes supported >70% b.p., suggesting taxonomic congruence among partitions (results not shown). However, the nuc18S, *psbA*, and *trnL-trnF* partitions contained at least one conflicting node >70% b.p. The nuc18S partition resolved *Sphagnum* and *Preissia* (a liverwort outgroup) as closer to the arthrodontous mosses than the nematodontous mosses at 75% b.p. The *psbA* partition resolved a clade, supported at 79% b.p. including of *Oedipodium*, *Andreaeobryum*, *Andreaea*, *Sphagnum*, and *Takakia*, within which the latter four taxa formed a clade supported by 82% b.p. The *trnL-trnF* partition contained the clade *Andreaea* plus *Oedipodium* supported by 74% b.p.

Maximum parsimony analyses of the combined dataset recovered a single optimal tree of length 4904 steps (ensemble consistency index (CI)= 0.386 (Kluge

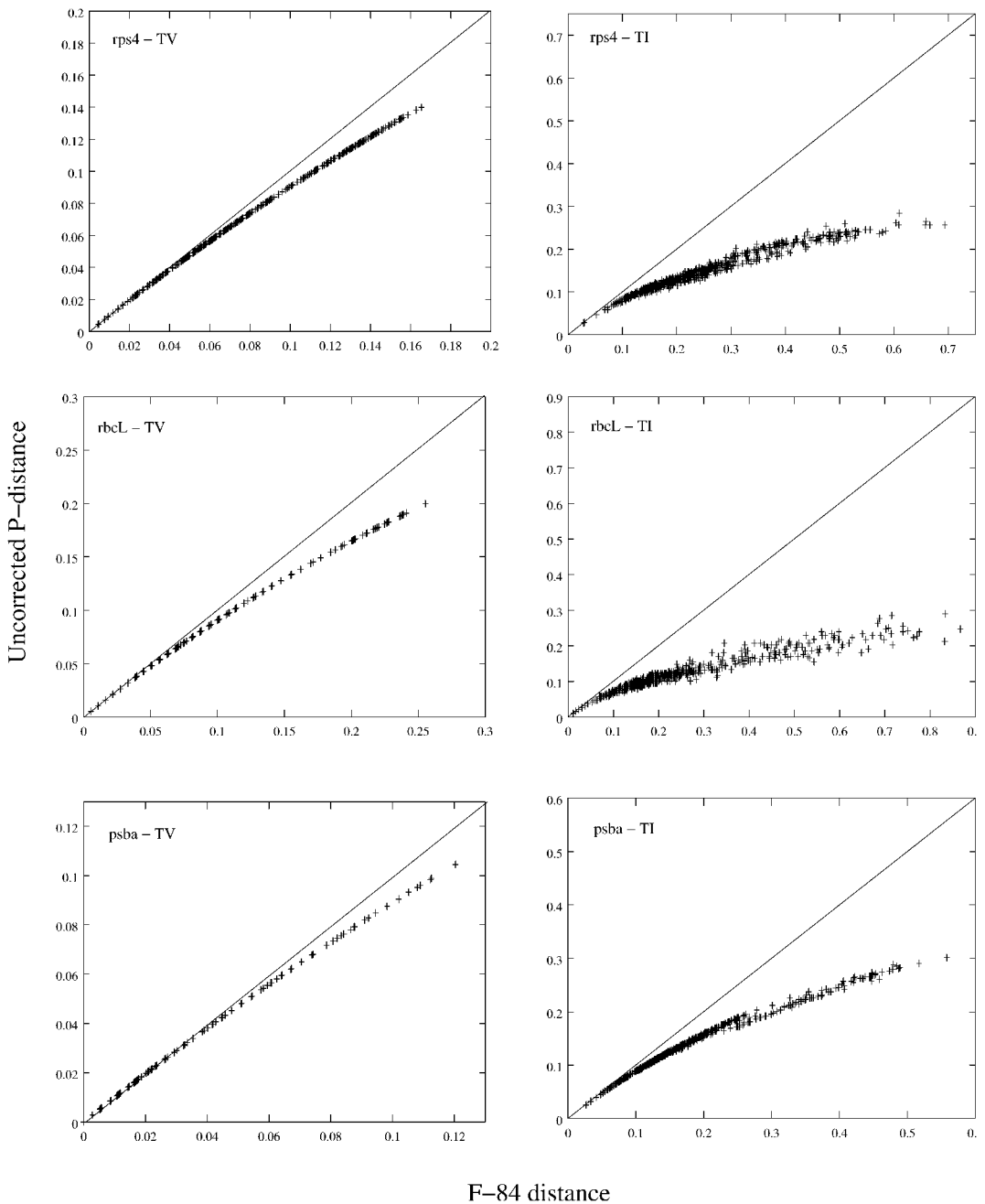


FIG. 1. Uncorrected P-distances versus F-84 corrected distances for transitions only (left-hand column) and transversions only (right-hand column) at third-codon positions of each protein-coding gene (*rps4*, *rbcL*, and *psbA*).

and Farris 1969), ensemble retention index (RI)= 0.52 (Farris 1989), ensemble rescaled consistency index (RC)= 0.203 (Farris 1989)). Figure 2 is the single MP tree with > 50% b.p. bootstrap proportions at each node. The ingroup taxa formed a highly supported (100% b.p.) clade with *Buxbaumia* forming the sister group to the remaining ingroup taxa with very low support (52% b.p.). The arthrodonotus mosses (*Di-*

physcium-Hookeria; 77% b.p.) compose a monophyletic sister-group to the remainder of the ingroup taxa, which form a weakly supported clade (56% b.p.). *Tetrarhis* was weakly supported (56% b.p.) as the sister group to a dichotomy between the polytrichaceous mosses (*Alophosia-Polytrichadelphus*; 97% b.p.) and a clade formed by *Oedipodium*, *Andreaobryum*, *Andreaea*, *Takakia*, and *Sphagnum* (78% b.p.). Within the latter

TABLE 2. Model selection results for each partition using the hierarchical likelihood ratio test as implemented in the program MrModeltest (Nylander 2002). GTR: General time-reversible, Rodriguez et al 1990; HKY: Hasegawa-Kishino-Yano, Hasegawa et al. 1985; SYM: model of Zharkikh 1994; K80: Kimura 1980. ¹ First and second codon positions, ² third codon positions, ³ non-coding region of *psbA* sequences. Base—base frequencies (A,C,G); Rmat—rate matrix (AC, AG, AT, CG, CT); Tratio—transversion ratio; Shape—value of α in gamma distribution; Pinvar—proportion of invariant characters.

Partition	Model	-ln likelihood	Optimized Parameters
combined	GTR+I+G	40817.9855	Base = (0.2768 0.1944 0.2389) Rmat = (1.4165 6.1193 1.0457 1.0247 10.2395) Shape = 0.7122 Pinvar = 0.5025
<i>nad5</i>	GTR+G	4644.4727	Base = (0.2754 0.2004 0.2078) Rmat = (1.7580 6.4359 0.2649 0.8741 8.5731) Shape = 0.5638 Pinvar = 0
<i>nad7</i>	HKY+G	3339.5808	Base = (0.3107 0.2193 0.2637) TRatio = 4.1730 Shape = 0.6581 Pinvar = 0
<i>nuc18s</i>	SYM+I+G	4637.8867	Base = equal Rmat = (1.1159 4.1196 0.7268 1.0141 8.6817) Shape = 0.6680 Pinvar = 0.7612
<i>nuc26s</i>	GTR+I+G	3702.8174	Base = (0.2394 0.2457 0.3256) Rmat = (0.8575 2.7919 0.6419 0.4307 5.0103) Shape = 0.643 Pinvar = 0.6597
<i>trnL-trnF</i>	GTR+G	1351.7063	Base = (0.3322 0.1762 0.2326) Rmat = (0.1281 5.9011 0.8502 0.0000 3.7145) Shape = 0.3728 Pinvar = 0
<i>rps4</i>	HKY+I+G	5491.1328	Base = (0.3812 0.1543 0.1757) TRatio = 3.9175 Shape = 0.9363 Pinvar = 0.2421
<i>rps4</i> (1+2) ¹	GTR+I+G	2677.3557	Base = (0.3749 0.1992 0.1597) Rmat = (1.3785 9.8921 0.4075 2.1786 7.5331) Shape = 0.9247 Pinvar = 0.3824
<i>rps4</i> (3) ²	GTR+G	2596.3743	Base = (0.4176 0.0576 0.1356) Rmat = (2.3931 6.3923 0.1221 1.0289 11.6828) Shape = 1.8605 Pinvar = 0
<i>rbcL</i>	GTR+I+G	9759.5049	Base = (0.2863 0.1561 0.2107) Rmat = (2.4746 6.6575 1.2028 3.3247 15.2472) Shape = 0.8207 Pinvar = 0.4616
<i>rbcL</i> (1+2)	SYM+I+G	3335.6284	Base = equal Rmat = (4.1881 2.4561 1.1587 3.7532 8.3061) Shape = 0.5126 Pinvar = 0.6550
<i>rbcL</i> (3)	GTR+I+G	5823.9897	Base = (0.3412 0.1062 0.0695) Rmat = (0.5387 7.2903 0.1383 0.0729 4.9001) Shape = 2.1593 Pinvar = 0.0960
<i>psbA</i>	GTR+I+G	6282.2539	Base = (0.2384 0.1981 0.2070) Rmat = (0.59453 8.3184 2.5202 0.2916 25.7391) Shape = 0.8459 Pinvar = 0.5361
<i>psbA</i> (1+2)	SYM+I+G	1628.0276	Base = equal Rmat = (1.6700 3.3215 0.5279 0.5592 17.5021) Shape = 0.7777 Pinvar = 0.8346
<i>psbA</i> (3)	GTR+G	3629.8254	Base = (0.2212 0.2295 0.0884) Rmat = (0.3451 11.8490 1.6441 0.0000 14.4130) Shape = 0.9921 Pinvar = 0
<i>psbA non-code</i> ³	K80+G	667.9110	Base = equal TRatio = 2.3001 Shape = 0.3636 Pinvar = 0

model to the data as model complexity increased. The relative rates of the eight regions (8-part model) were: 0.87 (*nad5*), 0.94 (*nad7*), 0.25 (*nuc18S*), 0.60 (*nuc26S*), 1.0 (*psbA*), 1.8 (*rbcL*), 2.4 (*rps4*), 1.0 (*trnL-trnF*).

The single most-likely tree under a homogeneous likelihood model across all partitions is presented in Fig. 3a. The homogeneous ML tree placed *Sphagnum* plus *Takakia* as the first diverging clade of the mosses. *Andreaobryum* and *Andreaea* were placed as the next most divergent group, followed by *Oedipodium*. The polytrichaceous mosses formed a clade, within which *Alophosia*, and then *Dendroligotrichum*, formed successive sister groups to *Polytrichadelphus* plus *Polytrichum*. In the sister group to the polytrichaceous clade, *Tetraphis*, followed by *Buxbaumia*, formed successive sister groups to the arthrodontous mosses. The topology within the arthrodontous mosses was identical to that obtained by equally-weighted parsimony (Fig. 2).

Bootstrap proportions (>50%), both ML- and Bayesian-based, and Bayesian posterior probabilities (>50%) for each node (as indicated in Fig. 3) are given in Table 3. ML bootstrap proportions under the homogeneous model, and Bayesian-based bootstrap proportions under the eight partition model, were very similar (within 5%) on branches for all but seven nodes. Support for the clade uniting *Haplomitrium*, *Pellia*, and *Porella* (node 2, Fig. 3a) was reduced by 10% in the Bayesian bootstrap when compared to the ML bootstrap. Similarly, support for the node including the *Polytrichales*, *Tetraphis*, *Buxbaumia*, and the arthrodontous mosses (node 8, Fig. 3a) was reduced from 72% to 63%. In contrast, several nodes gained a large increase in support when analyzed using the Bayesian methodology: *Tetraphis*, *Buxbaumia*, and the arthrodontous mosses (node 12, Fig. 3a) +7%; *Rhodobryum*, *Mielichhoferia*, and *Mnium* (node 24, Fig. 3a) + 18%; *Aulaconnium* and *Pyrrhobryum* (node 28, Fig. 3a) + 13%.

Bayesian bootstrap proportions under the 12-part model differed by greater than 5% from those under the 8-part model at 11 nodes. Most notably, support for the node uniting all mosses except *Sphagnum* and *Takakia* was increased to 90% (from 72%), the clade formed by *Oedipodium* and the remainder of the mosses (node 7, Fig. 3a) was significantly supported at 95% (from 88%), and the clade uniting *Sphagnum* and *Takakia* was supported by < 50% (from 84%).

Twenty-three nodes were significantly supported (i.e., >95%) by Bayesian posterior probability under all model permutations (Table 3). In comparison to the homogeneous Bayesian analysis, two clades gained a large increase (>5%) in posterior probability when analyzed under the 8-part model, namely, *Bartramia* plus the diplolepideous-alternate mosses (excl. *Hedwigia*) (node 22, Fig. 3a) increased by 13%, and the clade uniting *Orthodontium*, *Aulaconnium*, *Pyrrhobryum*, *Orthotrichum*, *Tetraplodon*, *Hookeria*, and *Brachythecium* (node 26,

Fig. 3a) increased by 16%. However, the latter of these clades was not supported >50% under 12-part heterogeneous analyses, while support for the former clade decreased by 12 and 13% in their Bayesian posterior probability, respectively. Two clades, firstly, that formed by *Orthodontium*, *Aulaconnium*, and *Pyrrhobryum* (node 27, Fig. 3a), and secondly, that formed by *Brachythecium*, *Hookeria*, *Orthotrichum*, and *Tetraplodon* (node 29, Fig. 3a), had lower posterior probabilities when analysed under the 8-part models (with and without RR) as compared to the 1-part (homogeneous) analysis (Table 3). Furthermore, these two clades were supported < 50% when analyzed under the 12-part models. The node uniting *Tetraphis*, *Buxbaumia*, and the arthrodontous mosses (node 12, Fig. 3a) was not significantly supported under the homogeneous Bayesian analysis (91%) but was under all heterogeneous analyses. Node 22 (Fig. 3a), as described above, was only significantly supported (95%) in the 8-part (without RR) Bayesian analyses.

The homogeneous 1-part and heterogeneous 8-part (with and without RR) Bayesian analyses all found maximum posterior probabilities for nodes compatible with the ML tree, except node 16 (Fig. 3a) which received < 50% posterior probability in the three analyses. In contrast, Bayesian posterior probabilities of the 12-part (with and without RR) supported clades not present in the ML tree or not supported by the 8-part analyses. In particular, there was < 50% Bayesian posterior probability for the sister relationship of *Timmia* to the clade formed by *Encalypta*, *Entosthodon*, and *Funaria*, in the ML bootstrap and 8-part Bayesian analyses. However, both 12-part Bayesian analyses resolved *Timmia* as the sister-group to the clade formed by the diplolepideous-alternate mosses and the haplolepideae (node 32, Fig. 3b), although with low posterior probability (67% and 72%). Furthermore, the 12-part heterogeneous analyses supported three novel clades not present in the ML tree: 1) *Rhodobryum*, *Mielichhoferia*, *Mnium*, *Orthodontium*, *Aulaconnium*, *Pyrrhobryum*, *Brachythecium*, and *Hookeria* (node 33, Fig. 3c: 66 and 69%), 2) *Orthodontium*, *Aulaconnium*, *Pyrrhobryum*, *Brachythecium*, and *Hookeria* (node 34, Fig. 3c: 99 and 100%), and 3) *Aulaconnium*, *Pyrrhobryum*, *Brachythecium*, and *Hookeria* (node 35, Fig. 3c: 100 and 100%).

The clade formed by *Sphagnum* and *Takakia* (node 4 Fig. 3a) was significantly supported (>95%) in the homogeneous and 8-part analyses but received < 50% posterior probability under the 12-part model. In the 12-part+RR heterogeneous analyses the tree with the highest posterior probability placed *Sphagnum* and *Takakia* sister taxon to the rest of the mosses ($p = 0.132$), while the tree with the second highest posterior placed *Sphagnum* alone as the sister taxon to the rest of the mosses ($p = 0.122$).

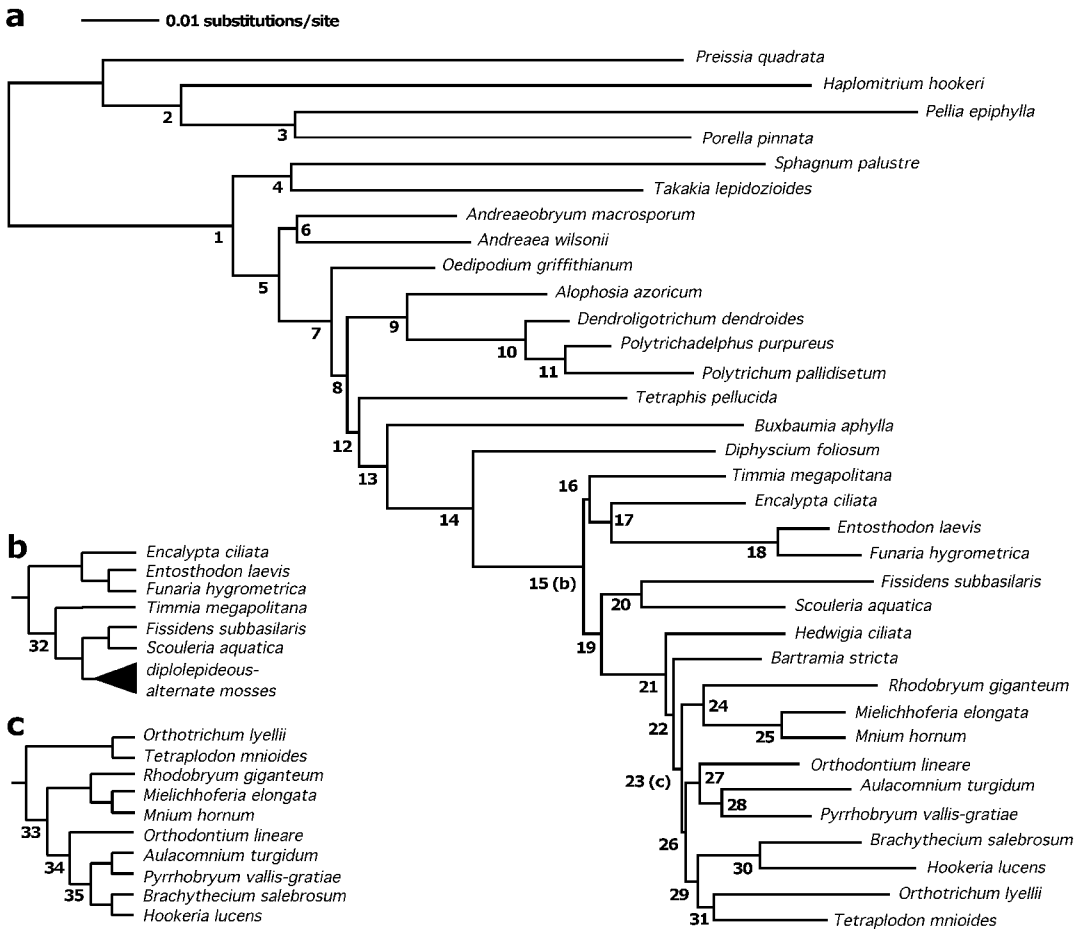


FIG. 3. a) The single optimal tree under maximum likelihood (GTR+I+G: general time-reversible substitution model, four discrete categories of gamma-distributed among-site rate heterogeneity, plus a proportion of invariant sites) found during 100 random taxon-addition heuristic search replicates with TBR branch-swapping (fixed parameter values are given in Tab. 2). Numbers below branches, or to the right of nodes, indicate nodes referred to in Tab. 3. (b) & (c) optimal topology rearrangements under 12-part heterogeneous Bayesian analysis.

DISCUSSION

Model Complexity and Selection. Application of the parsimony criterion to our data resulted in a phylogenetic hypothesis wherein *Sphagnum* and *Takakia* are derived from a common ancestor shared with *Andreaea* and *Andreaeobryum*, and together these taxa form a well-supported monophyletic clade (93% bootstrap) nested within the nematodontae (Fig. 2). Such relationships contradict all previously proposed phylogenetic concepts for the mosses (e.g., Vitt 1984; Beckert et al. 1999) including inferences from the analysis of morphological or multigene and multigenomic based molecular characters (Newton et al. 2000). Due to the lack of constraints at the amino-acid level for substitutions at third-positions of codons (e.g., Meyer 1994), and the higher frequency of transitions relative to transversions (Kimura 1980), transitions at third-positions of codons are those substitutions where homoplasy would be expected

to be greatest. Furthermore, comparisons of corrected versus uncorrected distances at third-positions suggests a high level of multiple-hits (substitutional saturation) at these sites. The absence of this novel relationship in subsequent analysis by transversion parsimony at third-positions (and also the ML based analyses) reveals that the signal was mainly in the form of transitions at third codon positions of protein-coding genes. We therefore conclude that support for the above novel phylogenetic hypothesis resulting from equally-weighted parsimony is most likely due to unsuitability (misspecification) of the implied model. In other words, the nesting of *Sphagnum* and *Takakia* within rather than sister to the main moss clade in equally-weighted parsimony is very likely an artifact.

In contrast to parsimony, model specification in the maximum likelihood framework is explicit. Increased model complexity results in a significantly better fit of

TABLE 3. Support indices for nodes identified on Fig. 3. Branch lengths—branch lengths of the optimal ML tree in numbers of substitutions per site; ML-b.p.—maximum likelihood bootstrap proportions >50%; bayes-b.p.—eight sub-model Bayesian bootstrap proportions >50%; 1-part—homogeneous single model Bayesian analysis; 8-part—eight sub-model Bayesian analysis employing P4; 11-part—eleven sub-model analysis employing P4; RR—relative rate parameter included. Nodes marked by an asterisk are alternative resolutions of the ML tree as indicated in the subtrees of Fig. 1b. N/A—not applicable (node not present in tree). “—” indicates <50% support.

node #	Branch lengths	ML-b.p.	Bayes-b.p. 8-part	Bayes-b.p. 12-part	1-part	8-part	8-part-RR	12-part	12-part-RR
1	0.0438	100	98	98	100	100	100	100	100
2	0.0106	99	89	77	100	100	100	100	100
3	0.0158	95	92	95	100	100	100	100	100
4	0.0079	86	84	—	100	99	99	—	—
5	0.0061	67	72	90	99	99	100	100	100
6	0.0026	—	63	61	86	86	90	78	85
7	0.0073	91	88	95	99	100	100	99	100
8	0.0022	72	63	61	99	99	100	100	100
9	0.0082	100	100	100	100	100	100	100	100
10	0.0162	100	100	100	100	100	100	100	100
11	0.0053	98	98	98	100	100	100	100	100
12	0.0017	52	59	53	91	96	95	95	95
13	0.0037	83	83	76	99	100	100	100	100
14	0.0117	100	99	98	100	100	100	100	100
15	0.0152	100	100	99	100	100	100	100	100
16	0.0007	—	—	—	—	—	—	N/A	N/A
17	0.0032	77	81	76	100	100	100	100	100
18	0.0226	100	100	100	100	100	100	100	100
19	0.0024	78	81	82	100	100	100	100	100
20	0.0057	100	100	99	100	100	100	100	100
21	0.0090	100	100	100	100	100	100	100	100
22	0.0011	—	—	—	82	95	94	83	81
23	0.0010	62	63	54	99	100	100	100	100
24	0.0032	66	84	94	100	100	100	100	100
25	0.0106	100	100	100	100	100	100	100	100
26	0.0007	—	—	—	64	80	80	N/A	N/A
27	0.0020	—	—	—	85	72	53	N/A	N/A
28	0.0028	61	74	74	99	100	100	100	99
29	0.0017	—	—	—	85	72	53	N/A	N/A
30	0.0083	100	99	100	100	100	100	100	100
31	0.0020	—	57	—	96	95	97	99	100
32*	—	—	—	—	N/A	N/A	N/A	67	72
33*	—	—	—	—	N/A	N/A	N/A	66	69
34*	—	—	—	51	N/A	N/A	N/A	99	100
35*	—	—	—	56	N/A	N/A	N/A	100	100

the model to the data in all comparisons as determined by the likelihood ratio test (i.e., 12-part+RR > 12-part > 8-part+RR > 8-part > homogeneous). The relative rate parameter among partitions as implemented in P4 had a substantial effect on model specification (the likelihood improved by >200 units in both comparisons) and, hence, posterior probabilities. Nevertheless, the addition of single parameters (other than the relative rate parameter (RR)) to the model was not tested individually; rather multiple parameters specific to a partition were added simultaneously. Hence, models may be over parameterized—an undesirable property leading to greater sampling variance (Swofford et al. 1996). A more thorough model specification than that applied here would test the addition of single parameters across partitions and combinations of partitions.

The necessity for careful model specification is highlighted by the support for the node uniting *Sphagnum*

and *Takakia* (node 4, Fig. 3a). Under ML bootstrap and 8-part heterogeneous Bayesian bootstrap, as well as 8-part Bayesian analyses, support for the sister relationship of *Sphagnum* and *Takakia* was high (86%, 84%, and 99%, respectively). However, when third positions of the protein coding genes were included as separately modeled partitions (12-part analyses) posterior probabilities and bootstrap proportions decreased to < 50%. This observation underlines the problematic nature of substitutions at the third-codon positions in our data set, particularly at deep nodes, and the necessity for careful model specification. In fact, the optimal relative rates of the three third-codon position partitions were $\times 3.6$, $\times 13.9$, and $\times 7.93$ that of the first- and second-codon positions for the *rps4*, *psbA*, and *rbcl* genes, respectively.

Heterogeneous Bayesian Analyses and the Bootstrap Bayesian posterior probabilities have the advantage that

their interpretation is straight-forward in the sense that they directly represent the probability of a hypothesis given the data (Lewis 2001). However, in molecular phylogenetic studies the investigator may also wish to know the expected repeatability of the hypothesis if or when additional data are obtained. This concern, along with the substantial type-1 error rates associated with posterior probabilities for relatively short branches, makes the bootstrap a valuable complementary metric for Bayesian phylogenetic analysis. In our study, several nodes consistently gained a significant (>95%) posterior probability while bootstrap proportions remained relatively low (<70%). For instance, the clade including polytrichaceous mosses, *Tetraphis*, *Buxbaumia*, and the arthrodontous mosses (node 8, Fig. 3a) was well supported under ML bootstrap (72%) and by posterior probability (99%). However, as model specification improved, bootstrap support for the node decreased to 63% (8-part) and 61% (12-part) even though posterior probabilities remained significant (100% for both model specifications). Similarly, the node uniting *Orthotrichum* and *Tetraplodon* (node 31, Fig. 3a), was significantly supported in all Bayesian analyses, and yet gained bootstrap support > 50% under only the 8-part Bayesian bootstrap, and then only at 57%. Support for these nodes, and others with similar disparities between posterior probabilities and the bootstrap, should be interpreted with caution.

Phylogenetic Relationships of the Mosses. Phylogenetic inferences based on an extensive sampling of genes from all three genomic compartments provide a well-resolved evolutionary history, with mostly well-supported relationships among the major lineages. Monophyly of the Bryophyta (sensu Buck and Goffinet 2000), and thus the inclusion of *Takakia*, is characterized by high levels of confidence. However, the placement of the root node of the mosses remains tentative, as demonstrated by the lack of support for the sister relationship of *Sphagnum* and *Takakia* under the most complex (12-part) Bayesian analysis. Except for this caveat, all ML and Bayesian analyses suggest *Takakia* and *Sphagnum* compose the first diverging lineage, followed by the origin of the lantern mosses (*Andreaea* and *Andreaobryum*). Peristomate mosses originated from a common ancestor with *Oedipodium* (an operculate but gymnostomous (lacking a peristome) moss), and the gradual modification of the peristome led to the evolution of the arthrodontous mosses from a nematodontous ancestor. Except for the relationships within the arthrodontous mosses, our topology is essentially congruent with the phylogenetic hypothesis proposed by Newton et al. (2000) based on a similar overall sampling of moss diversity and combined parsimony analyses of four of the gene regions used in this study (*rps4*, *trnL*, *rbcL*, and nuclear 18S rDNA).

Takakia, a genus of only two species, with a liver-

wort-like gametophyte (see Schuster 1997) but a moss sporophyte (Smith and Davison 1993; Renzaglia et al. 1997), is reconstructed in a rather basal position, but its exact affinities remain ambiguous. The phylogenetic relationships of *Takakia* have previously been formally tested by Hedderson et al. (1998; 18SrDNA), Newton et al. (2000; 18SrDNA + cpDNA), and Yatsentyuk (2001; cpDNA). In these studies, as well as in the present one, a close relationship to *Sphagnum* appears as the most likely or parsimonious hypothesis, but inferences based solely on chloroplast sequences suggest that *Takakia* is sister to all other mosses (Yatsentyuk 2001). *Takakia* and *Sphagnum* differ in the mode of sporangium dehiscence (single longitudinal spiral line versus a subapical horizontal one), the presence of seta versus pseudopodium, leaf development and mature structure, and stem anatomy (Crum 2001). In fact, Newton et al. (2000) did not find a single morphological synapomorphy that would unite *Takakia* and *Sphagnum*. Critical ultrastructural and developmental studies may provide characters needed to validate the sister-group relationship with *Sphagnum*, particularly in the absence of strong molecular support.

The affinities of *Andreaobryum* and *Andreaea* have remained a point of ambiguity in reconstructing the evolution of mosses (e.g., Newton et al. 2000). Our data resolve these two genera as sister-groups but without significant support. Although both taxa are similar in Gestalt and share a suite of morphological characters, they differ in important anatomical and developmental features, such as the shape of the sporophyte foot, mode of sporangium dehiscence, the presence of intercalary sporophyte growth, and timing of perichaeium development relative to sporophyte maturation (Murray 1988; Newton et al. 2000). Some of these conflicting characters-states could support alternative relationships, in particular that of *Andreaobryum* (but not *Andreaea*) to *Takakia* (Murray 1988). A common ancestry of *Andreaobryum* and *Andreaea* (Fig. 2b) was also supported by Newton et al. (2000) and Goffinet et al. (2001). Putative synapomorphies uniting these lineages include 1) dehiscence of the sporophyte along four longitudinal slits, and 2) multiseriate protonemata that 3) produce appendages not derived from side branch initials (Newton et al. 2000). Support for a common ancestry of *Andreaea* and *Andreaobryum* is weak to moderate in this and previous studies.

The implications of our results for morphological evolution in mosses include 1) a pseudopodium has arisen independently in *Sphagnum* and *Andreaea*, and 2) mucilage hairs of *Andreaobryum* and *Takakia* are not homologous (contra Schuster 1997). Considering that stomata are lacking in *Takakia*, *Andreaea*, and *Andreaobryum* (Crum 2001), our phylogeny also suggests that the stomata in *Sphagnum* may not be homologous to those found on the capsule wall of other mosses. This

hypothesis was presented by Boudier (1988), who argued that the stomata in *Sphagnum* were not involved in gas exchange but rather play an important role in spore dispersal and that these differentiate in the capsule wall at a later stage than true stomata. The implications of this hypothesis are profound, since the absence of stomata may be plesiomorphic for mosses, and hence the stomata of mosses cannot be considered homologous to those of vascular plants (Mishler and Churchill 1984). The axial columella in the sporangium of mosses is typically cylindrical, but in *Takakia*, *Sphagnum*, *Andreaea*, and *Andreaebryum* it is dome-shaped and overarched by the archesporium. A similar columella is present in hornworts, the fossil moss *Sporogonites* Halle, and the early polysporangiophyte, *Horneophyton* (Kidson & Lang) Barghoorn & Darrah (Kenrick and Crane 1997), and hence is evidently plesiomorphic in mosses.

Newton et al. (2000) and Goffinet et al. (2001) recently suggested that *Oedipodium* may hold a crucial position in the phylogeny of mosses as sister to the clade of peristomate mosses. It was previously considered closely related to Funariaceae (Vitt 1984). The hypothesis that *Oedipodium* is sister to peristomate mosses is well supported by our data. *Oedipodium* is a monospecific genus characterized by the lack of a peristome. It shares with its sister group a sporangial dehiscence involving the loss of an apical lid (operculum). Other synapomorphies for this clade include a filamentous protonema, cylindrical columella, terminal position of the antheridia, and imperforate hydroids (Newton et al. 2000). Whether peristomes evolved prior to the divergence of *Oedipodium* and were subsequently lost in the latter (as is the case in many mosses lineages, Vitt 1981) cannot presently, and may never, be determined. Due to its gymnostomous capsule, *Oedipodium* cannot contribute to the resolution of peristome evolution per se, but examination of the cell divisions in the layers that form peristomes in other mosses may provide insight into polarity of developmental patterns in these cell layers.

Peristomate mosses form a clade supported by low to moderate bootstrap proportions, but high posterior probabilities. The clade, which accommodates the vast majority of mosses, can at present only be defined by the presence of a peristome, as no other synapomorphy is known to distinguish it from its sister-group, *Oedipodium*. A sister-group relationship between arthrodontous (incl. *Diphyscium*) and nematodontous mosses, as suggested by Goffinet et al. (2001), is not supported here. Instead, the nematodontous lineages (i.e., the Polytrichaceae and the Tetrarhizaceae) form a paraphyletic group.

Although the Polytrichaceae and Tetrarhizaceae have teeth composed of whole cells, their peristomes differ in ontogeny and architecture at maturity. The

Polytrichaceae typically bear 64 teeth and the amphithecium undergoes an additional anticlinal division prior to the differentiation of the IPL (Wenderoth 1931). The peristome of *Tetraphis* is composed of four massive teeth, and its ontogeny is similar to that of arthrodontous mosses (i.e., lacking the additional anticlinal division), at least in the early stages (Shaw and Anderson 1988). Mishler and Churchill (1984) had previously argued for the paraphyly of the nematodontous mosses, although their phylogenetic hypothesis resolved *Polytrichum* and not *Tetraphis* as sister to the arthrodontous mosses on the basis of airspaces occurring in the capsule of the Polytrichaceae and the latter. Our results concur with those obtained by Hyvönen et al. (1998) and Newton et al. (2000) whereby *Tetraphis* shares a common ancestor with the arthrodontous mosses (incl. *Buxbaumia* and *Diphyscium*). Newton et al. (2000) found a single synapomorphy for this clade, namely the presence of gametophyte transfer cells with labyrinthine outgrowth on the inner tangential walls of the cells. Paraphyly of nematodontous taxa would suggest that the nematodontous architecture of the peristome is ancestral in peristomate mosses. Whether the additional division of the amphithecium in *Polytrichum*, and the symmetry of the anticlinal divisions in the IPL are plesiomorphic for this clade of bryophytes, or autapomorphic for the Polytrichaceae cannot be determined in the absence of ontogenetic studies of the sporophyte of *Oedipodium* or other basal mosses.

The genus *Buxbaumia* is characterized by a reduced gametophyte and massive sporophytes. More significantly, from a phylogenetic perspective, its peristome combines nematodontous and arthrodontous elements (Edwards 1984). Vitt (1984) considered *Buxbaumia* allied to arthrodontous mosses because the innermost peristome teeth consist of cell plates rather than whole cells. *Diphyscium* has a differentiated gametophyte composed of a leafy stem, and a peristome composed of two rows of teeth, all composed of cell wall remnants (Edwards 1984). Although these two genera have long been considered closely related, recent inferences from molecular characters (Hyvönen et al. 1998 [18SrDNA only]; Beckert et al. 1999; Newton et al. 2000; Goffinet et al. 2001) converged toward a hypothesis of para- or polyphyly of the Buxbaumiineae sensu Vitt (1984), as previously suggested by Mishler and Churchill (1984). *Diphyscium* is consistently resolved as a sister-group to the remaining arthrodontous mosses. By contrast, the affinities of *Buxbaumia* either have been ambiguous (Hyvönen et al. 1998—based on *rbcL* data), or with the Tetrarhizaceae (Newton et al. 2000; Goffinet et al. 2001). Our analyses yield moderate to high support for the placement of *Buxbaumia*, and consistently high support for that of *Diphyscium*. Monophyly of a clade rooted with *Buxbaumia* is congruent with the

presence of a significant deletion in the *rps4-trnA* spacer in all these taxa (Goffinet et al. 2001).

Within arthrodontous mosses our results suggest that the Funariaceae are sister to a clade comprising two monophyletic lineages, the Haplolepeidae and diplolepeidae mosses with alternate peristomes. This hypothesis is congruent with that proposed by Newton et al. (2000) based on characters from the nuclear and plastid genomes, but differs from inferences made solely based on chloroplast (Goffinet et al. 2001) or mitochondrial data (Beckert et al. 1999). The clade composed of the Haplolepeidae and the diplolepeidae-alternate taxa currently lacks a known morphological synapomorphy. Although both lineages share the occurrence of an asymmetric division in their IPL (Shaw et al. 1989a, b), such asymmetric divisions also occur in *Diphyscium* (Shaw et al. 1987) and maybe even in *Tetraphis* (Shaw and Anderson 1988).

Recent studies by Cox and Hedderson (1999), Newton et al. (2000), and Goffinet et al. (2001) converged on highlighting the phylogenetic significance of the genus *Timmia* in the early evolutionary history of arthrodontous mosses. The proposed hypotheses were, however, incongruent in terms of the actual affinities of *Timmia*: sister to all mosses except *Funaria* (Cox and Hedderson 1999; Newton et al. 2000), or sister to a clade combining *Encalypta* and *Funaria* (Goffinet et al. 2001). The peristome of *Timmia* is diplolepeidae, and its endostome is composed of a pleated membrane topped by 64 narrow appendages. Cox and Hedderson (1999), Goffinet and Cox (2000), and Cox et al. (2000), regarded the peristome of *Timmia* as of the opposite type, whereas Vitt (1984) implicitly interpreted the peristome to be alternate, since he placed the Timmiaceae in the Bryineae. Despite the significantly larger sampling of DNA sequences, the affinities of *Timmia* cannot be resolved here: its position varies among analyses (see above) and in all cases support is very low to moderate at best.

The affinities of *Encalypta* appear to lay with the Funariaceae. A sister-group relationship between the Encalyptaceae and the Funariaceae is consistently resolved and supported here by moderate bootstrap proportions and maximal posterior probabilities (node 17, Table 2). The remaining arthrodontous mosses compose a monophyletic lineage characterized by moderate bootstrap proportions and high posterior probabilities. Within this clade, mosses with a haplolepeidae peristome compose the sister group to diplolepeidae mosses with an alternate arrangement of teeth and segments. A shared ancestry between mosses with a haplolepeidae and a diplolepeidae-alternate peristome was hypothesized by Newton et al. (2000; based on molecular data only), but was argued against by Beckert et al. (1999) and Goffinet et al. (2001). Monophyly of these two lineages is strongly supported by our data, and bootstrap propor-

tions for their sister-group relationship are moderate, although posterior probabilities are very high (node 19, Table 2). Whether *Timmia* is sister to the *Funaria-Encalypta* clade or sister to the haplolepeidae-diplolepeidae alternate clade, the most parsimonious interpretation of its peristome is that it is of the opposite type. Indeed, the peristome is opposite in *Funaria* and *Encalypta* (Vitt 1984) as well as in the Haplolepeidae (Vitt et al. 1998). Consequently, this peristome type likely represents the ancestral architecture from which the alternate arrangement of teeth and segments are derived, as suggested by Vitt (1984).

The topology best supported by our analyses agrees in many details with results of previous research but our study was based on the most extensive sampling of molecular characters to date, and provides considerably greater support for relationships than previous studies. Nevertheless, it is remarkable that despite the amount of nucleotide data applied to the problem some of the internal branches are so short that ambiguities remain. Of particular importance for future research are the relationship between *Sphagnum* and *Takakia*, the position of *Timmia*, and topological details among acrocarpous mosses most closely related to the pleurocarps.

ACKNOWLEDGEMENTS. This research was supported by NSF grants no. DEB-0089131 to A.J.S. and DEB-0089633 to B.G. The authors wish to thank Peter Foster, John Huelsenbeck, and Fredrik Ronquist for making their software freely available to us.

LITERATURE CITED

- ALFARO, M. E., S. ZOLLER, and F. LUTZONI. 2003. Bayes or bootstrap? A simulation study comparing the performance of Bayesian Markov chain Monte Carlo sampling and bootstrapping in assessing phylogenetic confidence. *Molecular Biology and Evolution* 20: 255-266.
- BECKERT, S., H. MUHLE, D. PRUCHNER, and V. KNOOP. 2001. The mitochondrial *nad2* gene as a novel marker locus for phylogenetic analysis of early land plants: a comparative analysis in mosses. *Molecular Phylogenetics and Evolution* 18: 117-126.
- , S. STEINHAUSER, H. MUHLE, and V. KNOOP. 1999. A molecular phylogeny of the bryophytes based on nucleotide sequences of the mitochondrial *nad5* gene. *Plant Systematics and Evolution* 218: 179-192.
- BOUDIER P. 1988. Différenciation structurale de l'épiderme du sporogone chez *Sphagnum fimbriatum* Wilson. *Annales des Sciences Naturelles, Botanique* 8: 143-156.
- BROTHERUS V. A. 1924-5. Musci (Laubmoose). III. Unterklasse Bryales: II. Spezieller Teil. Pp. 277-700 in *Die Natürlichen Pflanzenfamilien*, ed. A. Engler. Leipzig: Engelmann.
- BUCK, W. R. 1980. A generic revision of the Entodontaceae. *Journal of the Hattori Botanical Laboratory* 48: 71-159.
- and H. CRUM. 1978. An evaluation of the familial limits among the genera traditionally aligned with the Thuidaceae and Leskeaceae. *Contributions from the University of Michigan Herbarium* 17: 55-69.
- and B. GOFFINET. 2000. Morphology and classification of the mosses. Pp. 71-123 in *Bryophyte biology*, eds. A. J. Shaw and B. Goffinet. Cambridge: Cambridge University Press.
- COX, C. J. and T. A. J. HEDDERSON. 1999. Phylogenetic relationships among the ciliate arthrodontous mosses: evidence from chlo-

- roplast and nuclear DNA sequences. *Plant Systematics and Evolution* 215: 119–139.
- , B. GOFFINET, A. E. NEWTON, A. J. SHAW, and T. A. J. HEDDERSON. 2000. Phylogenetic relationships among the diplolepidous-alternate mosses (Bryidae) inferred from nuclear and chloroplast DNA sequences. *The Bryologist* 103: 224–240.
- CRANDALL-STOTLER, B. and R. E. STOTLER. 2002. Morphology and classification of the Marchantiophyta. Pp. 21–70 in *Bryophyte biology*, eds. A. J. Shaw and B. Goffinet. Cambridge: Cambridge University Press.
- CROSBY, M. R., R. E. MAGILL, B. ALLEN, and S. HE. 1999. *Checklist of the mosses*. St. Louis: Missouri Botanical Garden.
- CRUM, H. A. 2001. *Structural diversity of bryophytes*. Ann Arbor: University of Michigan Herbarium.
- DOYLE, J. J. and J. L. DOYLE. 1987. A rapid DNA isolation for small quantities of fresh material. *Phytochemical Bulletin* 19: 11–15.
- EDWARDS, S. R. 1984. Homologies and inter-relationships of moss peristomes. Pp. 658–695 in *New manual of bryology*, vol. 2, ed. R. M. Schuster. Nichinan: Hattori Botanical Laboratory.
- EDWARDS, K., C. JOHNSTONE, and C. THOMPSON. 1991. A simple and rapid method for the preparation of plant genomic DNA for PCR analysis. *Nucleic Acids Research* 19: 1349.
- FARRIS, J. S. 1989. The retention index and the rescaled consistency index. *Cladistics* 5: 417–419.
- FELSENSTEIN, J. S. 1984. Distance methods for inferring phylogenies: a justification. *Evolution* 38: 16–24.
- . 1985. Confidence-limits on phylogenies: an approach using the bootstrap. *Evolution* 39: 783–791.
- FLEISCHER, M. 1904–23. *Die Musci der Flora von Buitzenborg (Zugleich Laubmoosflora von Java)*, Vols. 1–4. Leiden: Brill.
- FOSTER, P. 2002. P4—software and manual. London: Natural History Museum. <http://www.nhm.ac.uk/zoology/external/p4.htm>
- GARBARY, D. J., K. S. RENZAGLIA, and J. G. DUCKETT. 1993. The phylogeny of the green plants: a cladistic analysis based on male gametogenesis. *Plant Systematics and Evolution* 188: 237–269.
- GOFFINET, B. 2000. Origin and the phylogenetic relationships of the Bryophytes. Pp. 124–149 in *Bryophyte biology*, eds. A. J. Shaw and B. Goffinet. Cambridge: Cambridge University Press.
- and C. J. COX. 2000. Phylogenetic relationships among basal-most arthrodontous mosses with special emphasis on the evolutionary significance of the Funariineae. *The Bryologist* 103: 212–223.
- , ———, A. J. SHAW, and T. A. J. HEDDERSON. 2001. The bryophyta (mosses): systematic and evolutionary inferences from an *rps4* gene (cpDNA) phylogeny. *Annals of Botany* 87: 191–208.
- , J. SHAW, L. E. ANDERSON and B. D. MISHLER. 1999. Peristome development in mosses in relation to systematics and evolution. V. Diplolepidaeae: Orthotrichaceae. *The Bryologist* 102: 581–594.
- HASEGAWA, M., H. KISHINO, and T. YANO. 1985. Dating of the human-ape splitting by a molecular clock of mitochondrial DNA. *Journal of Molecular Evolution* 32: 443–445.
- HEDDERSON, T. A., R. CHAPMAN, and C. J. COX. 1998. Bryophytes and the origins and diversification of land plants: new evidence from molecules. Pp. 65–77 in *Bryology for the twenty-first century*, eds. J. W. Bates, N. W. Ashton, and J. G. Duckett. Leeds: Maney Publishing.
- , ———, and W. L. ROOTES. 1996. Phylogenetic relationships of bryophytes inferred from nuclear-encoded rRNA gene sequences. *Plant Systematics and Evolution* 200: 213–224.
- HILLIS, D. M. and J. J. BULL. 1993. An empirical test of bootstrapping as a method for assessing confidence in phylogenetic analysis. *Systematic Biology* 42: 182–192.
- HUELSENBECK, J. P. and F. RONQUIST. 2001. MrBayes version 2.01. Available from the authors: <http://morphbank.ebc.uu.se/mrbayes3/info.php>
- and ———. 2002. MrBayes version 3.0B. Available from the authors: <http://morphbank.ebc.uu.se/mrbayes3/info.php>
- , B. LARGET, R. E. MILLER, and F. RONQUIST. 2002. Potential application and pitfalls of Bayesian inference of phylogeny. *Systematic Biology* 51: 673–688.
- HYVÖNEN, J., T. A. HEDDERSON, G. L. SMITH MERRILL, J. G. GIBBINS, and S. KOSKINEN. 1998. On phylogeny of the Polytrichales. *The Bryologist* 101: 489–504.
- KENRICK P. and P. CRANE 1997. *The origin and early diversification of land plants. A cladistic study*. Washington DC: Smithsonian Institution Press.
- KIMURA, M. 1980. A simple method for estimating evolutionary rate of base substitution through comparative studies of nucleotide sequences. *Journal of Molecular Evolution* 16: 111–120.
- KINDBERG, N. C. 1897. *Genera of European and Northern American Bryineae (Mosses) synoptically disposed*. Göteborg: Bonniers Boktryckeri Aktiebolag.
- KLUGE, A. G. and J. S. FARRIS. 1969. Quantitative phyletics and the evolution of Anurans. *Systematic Zoology* 18: 1–32.
- LEWIS, L., B. D. MISHLER, and R. VILGALYS. 1997. Phylogenetic relationships of the liverworts (Hepatitaceae), a basal embryophyte lineage, inferred from nucleotide sequence data of the chloroplast gene *rbcL*. *Molecular Phylogenetics and Evolution* 7: 377–393.
- LEWIS, P. 2001. Phylogenetic systematics turns over a new leaf. *Trends in Ecology and Evolution* 16: 30–37.
- MEYER, A. 1994. Shortcomings of the cytochrome b gene as a molecular marker. *Trends in Evolution and Ecology* 9: 278–280.
- MISHLER, B. D. and S. P. CHURCHILL. 1984. A cladistic approach to the phylogeny of the “bryophytes”. *Brittonia* 36: 406–424.
- MITTEN, W. 1859. Musci Indiae Orientalis. An enumeration of the mosses of the East Indies. *Journal of the Proceedings of the Linnean Society (London), Supplement Botany* 1: 1–171.
- MURRAY, B. M. 1998. Systematics of the Andreaopsida (Bryophyta): two orders with links to *Takakia*. *Beiheft zur Nova Hedwigia* 90: 289–336.
- NEWTON, A. E., C. J. COX, J. G. DUCKETT, J. WHEELER, B. GOFFINET, B. D. MISHLER, and T. A. J. HEDDERSON. 2000. Evolution of the major moss lineages. *The Bryologist* 103: 187–211.
- NICKRENT D. L., C. L. PARKINSON, J. D. PALMER, and R. J. DUFF. 2000. Multigene phylogeny of the land plants with special reference to bryophytes and the earliest land plants. *Molecular Biology and Evolution* 17: 1885–1895.
- NYLANDER, J. A. A. 2002. MrModeltest—version 1.1b. Available from the author. <http://www.ebc.uu.se/systzoo/staff/nylander.html>
- PALISOT DE-BEAUVOIS, A. M. F. J. 1805. *Prodrome des cinquième et sixième familles de l'aéthéogamie. Les Mousses. Les lycopodes*. Paris: De Fournier Fils.
- PHILIBERT, H., 1884–1902. De l'importance du péristome pour les affinités naturelles des mousses. *Revue Bryologique* 11: 49–52, 65–72. Etudes sur le péristome. *Revue Bryologique* 11: 81–87; 12: 67–77, 81–85; 13: 17–27, 81–86; 14: 9–11, 81–90; 15: 6–12, 24–28, 37–44, 50–56, 65–69, 90–93; 16: 1–9, 39–44, 67–77; 17: 8–12, 25–29, 38–42.
- RENZAGLIA, K. S., R. J. DUFF, D. L. NICKRENT, and D. J. GARBARY. 2000. Vegetative and reproductive innovations of early land plants: implications for a unified phylogeny. *Philosophical Transactions of the Royal Society of London, Series B—Biological Sciences* 355: 769–793.
- , K. D. MCFARLAND, and D. K. SMITH. 1997. Anatomy and ultrastructure of the sporophyte of *Takakia ceratophylla* (Bryophyta). *American Journal of Botany* 84: 1337–1350.
- RODRIGUEZ, F., J. L. OLIVER, A. MARIN, and J. R. MEDINA. 1990.

- The general stochastic model of nucleotide substitution. *Journal of Theoretical Biology* 142: 485–501.
- SCHIMPER, W. P. 1853–55. Pleurocarpae (in part). Pp. 535–622 in *Bryologia Europaea seu generum muscorum Europaeorum monographice illustrata*. vol. VI, ed. P. Bruch, W. P. Schimper, and T. Gumbel. W. P. Schimper. Stuttgartiae: Schweizerbart.
- SCHUSTER R. M. 1997. On *Takakia* and the phylogenetic relationships of the Takakiales. *Novae Hedwigia* 64: 281–310.
- SHAW, A. J. 1986. Peristome structure in the Orthotrichales. *Journal of the Hattori Botanical Laboratory* 60: 119–136.
- and L. E. ANDERSON. 1988. Peristome development in mosses in relation to systematics and evolution. II. *Tetraphis pellucida* (Tetraphidaceae). *American Journal of Botany* 75: 1019–1032.
- , ———, and B. D. MISHLER. 1987. Peristome development in mosses in relation to systematics and evolution. I. *Diplazium foliosum* (Buxbaumiaceae). *Memoirs of the New York Botanical Garden* 45: 55–70.
- , ———, and ———. 1989a. Peristome development in mosses in relation to systematics and evolution. III. *Funaria hygrometrica*, *Bryum pseudocapillare*, and *B. bicolor*. *Systematic Botany* 14: 24–36.
- , B. D. MISHLER, and L. E. ANDERSON. 1989b. Peristome development in mosses in relation to systematics and evolution. IV. Haplolepidaceae: Ditrichaceae and Dicranaceae. *The Bryologist* 92: 314–325.
- SHOEMAKER, J. S., I. S. PAINTER, and B. S. WEIR. 1999. Bayesian statistics in phylogenetics: a guide for the uninitiated. *Trends in Genetics* 15: 354–358.
- SMITH, D. K. and P. G. DAVIDSON. 1993. Antheridia and sporophytes in *Takakia ceratophylla* (Mitt.) Groll: evidence for reclassification among the mosses. *Journal of the Hattori Botanical Laboratory* 73: 263–271.
- SUSUKI, Y., G. V. GLAZKO, and M. NEI. 2002. Overcredibility of molecular phylogenies obtained by Bayesian phylogenetics. *Proceeding of the National Academy of Sciences USA* 99: 16138–16143.
- SWOFFORD, D. L. 2002. PAUP*—Phylogenetic Analyses Using Parsimony (* and Other Methods). Version 4. Sunderland: Sinauer Associates.
- , G. J. OLSEN, P. J. WADDELL, and D. M. HILLIS. 1996. Phylogenetic inference. Pp. 407–514 in *Molecular systematics* eds. D. M. Hillis, C. Moritz, and B. K. Mable. Sunderland: Sinauer Associates.
- VITT, D. H. 1981. Adaptive modes of the moss sporophyte. *The Bryologist* 84: 166–186.
- . 1984. Classification of the Bryopsida. Pp. 676–759 in *New manual of bryology*, vol. 2, ed. R. M. Schuster. Nichinan: Hattori Botanical Laboratory.
- , B. GOFFINET, and T. HEDDERSON. 1998. The ordinal classification of mosses: questions and answers for the 1990's. Pp. 113–123 in *Bryology for the twenty-first century*, eds. J. W. Bates, N. W. Ashton, and J. G. Duckett. Leeds: Maney Publishing.
- WENDEROTH, H. 1931. Beiträge zur Kenntniss des Sporophyten von *Polytrichum juniperinum* Willdenow. *Planta* 14: 344–385.
- WILLIAMS, T. and C. KELLEY. 1999. GnuPlot version 3.7.1—software and documentation. <http://sourceforge.net/projects/gnuplot>.
- YATSENTYUK, S. P. 2001. *Molecular Phylogeny of the Bryophyta and Lycopodiophyta, according to results from some sequences of chloroplast DNA*. Ph.D. Dissertation, Moscow State University.
- ZHARKIKH, A. 1994. Estimation of evolutionary distances between nucleotide sequences. *Journal of Molecular Evolution* 39: 315–329.
- Allophosia azoricum*: 18S -, 26S AY330424, nad5 AY312867, nad7 AY330453, trnL-F -, rps4 AY330476, rbcL AY312924, psbA AY312891.
- Andreaea wilsonii*: 18S AY330416, 26S AY330425, nad5 AY312868, nad7 AY330454, trnL-F AY312939, rps4 AY330477, rbcL AY312925, psbA AY312892.
- Andreaebryum macrosporum*: 18S AJ275005, 26S AY330426, nad5 -, nad7 -, trnL-F -, rps4 AF306953, rbcL AF231059, psbA AY312893.
- Aulacomnium turgidum*: 18S AF023687, 26S AY330427, nad5 AY312869, nad7 AY330455, trnL-F AF023728, rps4 AF023809, rbcL AJ275180, psbA AY312894.
- Bartramia stricta*: 18S AF023698, 26S AY330428, nad5 AY312870, nad7 AY330456, trnL-F AF023756, rps4 AF023799, rbcL AY312926, psbA AY312895.
- Brachythecium salebrosum*: 18S AY330417, 26S AY330429, nad5 AY312871, nad7 AY330457, trnL-F AF161120, rps4 AF143027, rbcL AY312927, psbA AY312896.
- Buxbaumia aphylla*: 18S Y17603, 26S AY330430, nad5 AY312872, nad7 -, trnL-F AF231909, rps4 AF306959, rbcL AF231062, psbA AY312897.
- Dendroligotrichum dendroides*: 18S AY330418, 26S AY330431, nad5 AY312873, nad7 AY330458, trnL-F AY312940, rps4 AF208420, rbcL AF208411, psbA AY312898.
- Diplazium foliosum*: 18S Y17765, 26S AY330432, nad5 AY312874, nad7 AY330459, trnL-F AF229891, rps4 AJ251065, rbcL AY312928, psbA AY312899.
- Encalypta ciliata*: 18S AF223011, 26S AY330433, nad5 AY312875, nad7 AY330460, trnL-F AF229897, rps4 AF223040, rbcL AY312929, psbA AY312900.
- Entosthodon laevis*: 18S AY330419, 26S AY330434, nad5 AY312876, nad7 AY330461, trnL-F AY312941, rps4 AY330478, rbcL AY312930, psbA AY312901.
- Fissidens sub-silaris*: 18S AF223027, 26S AY330435, nad5 AY312877, nad7 AY330462, trnL-F AF229913, rps4 AF223056, rbcL AF231304, psbA AY312902.
- Funaria hygrometrica*: 18S X74114, 26S AY330436, nad5 Z98959, nad7 AY330463, trnL-F AF231175, rps4 AF023776, rbcL AF005513, psbA AY312903.
- Haplomitrium hookeri*: 18S Y19006, 26S AY330437, nad5 -, nad7 -, trnL-F AY312942, rps4 AJ251064, rbcL U87072, psbA AY312904.
- Hedwigia ciliata*: 18S AJ275010, 26S AY330438, nad5 Z98966, nad7 AY330464, trnL-F AF233587, rps4 AJ251309, rbcL AF231073, psbA AY312905.
- Hookeria lucens*: 18S AJ243168, 26S AY330439, nad5 Z98969, nad7 AY330465, trnL-F AF215906, rps4 AJ251316, rbcL AY312931, psbA AY312906.
- Miulichoferia elongata*: 18S AF023708, 26S AY330440, nad5 AY312878, nad7 -, trnL-F AF023766, rps4 AF023793, rbcL AF232693, psbA AY312907.
- Mnium hornum*: 18S X80985, 26S AY330441, nad5 AY312879, nad7 -, trnL-F AF182360, rps4 AF023796, rbcL AF226820, psbA AY312908.
- Oedipodium griffithianum*: 18S AF228668, 26S AY330442, nad5 AY312880, nad7 AY330466, trnL-F AF246290, rps4 AF306968, rbcL AY312932, psbA AY312909.
- Orthodontium lineare*: 18S AF023697, 26S AY330443, nad5 AY312881, nad7 AY330467, trnL-F AF023768, rps4 AF023800, rbcL AJ275174, psbA AY312910.
- Orthotrichum lyellii*: 18S AF025291, 26S AY330444, nad5 AY312882, nad7 AY330468, trnL-F AF023727, rps4 AF023814, rbcL AF005536, psbA AY312911.
- Pellia epiphylla*: 18S X80210, 26S AF226030, nad5 -, nad7 -, trnL-F -, rps4 AY330479, rbcL U87085, psbA AY312912.
- Polytrichadelphus purpureus*: 18S AY330420, 26S -, nad5 AY312883, nad7 AY330469, trnL-F AY312943, rps4 AY330480, rbcL AY312933, psbA AY312913.
- Polytrichum pallidisetum*: 18S AY330421, 26S AY330445, nad5 AY312884, nad7 AY330470, trnL-F AY312944, rps4 AF306956, rbcL AY312934, psbA AY312914.
- Porella pinnata*: 18S AY330422, 26S AY330446, nad5 -, nad7 -, trnL-F AY312945, rps4 AY330481, rbcL U87088, psbA AY312915.
- Preissia quadrata*: 18S X80211, 26S AY330447, nad5 -, nad7 -, trnL-F AY312946, rps4 AY330482, rbcL AY312935, psbA AY312916.
- Pyrrobryum vallis-gratiae*: 18S AF023695, 26S AY330448, nad5 AY312885, nad7 AY330471, trnL-F AF023754, rps4 AF023825, rbcL AJ275179, psbA AY312917.
- Rhodobryum giganteum*: 18S AF02369, 26S AY330449, nad5 AY312886, nad7 -, trnL-F AF023737, rps4 AF023789, rbcL AJ275176, psbA AY312918.
- Scouleria aquatica*: 18S AF023684, 26S AY330450, nad5 AY312887, nad7 AY330472, trnL-F AF023723, rps4 AF023780, rbcL AF226822, psbA AY312919.
- Sphagnum palustre*: 18S Y11370, 26S AY330451, nad5 AY312888, nad7 AY330473, trnL-F AF192634, rps4 AF231892, rbcL AF231887, psbA AY312920.
- Takakia lepidozoides*: 18S AJ269686, 26S AF197061,

APPENDIX 1

GenBank accession numbers of sequences used in the study in the order: nuclear 18S rDNA, nuclear 26S rDNA, nad5, nad7, trnL-trnF, rps4, rbcL, and psbA.

nad5 AY312889, *nad7* AJ309978, *trnL-F* AY312947, *rps4* AF306950, *AF023691*, *26S -*, *nad5 -*, *nad7* AY330474, *trnL-F* AF023730, *rps4*
rbcL AY312936, *psbA* AY312921. ***Tetraphis pellucida***: 18S U18527, *AF023804*, *rbcL* AY312937, *psbA* AY312922. ***Timmia megapolitana***:
26S AF226033, *nad5* AJ224855, *nad7 -*, *trnL-F* AF231908, *rps4* 18S AY330423, 26S AY330452, *nad5* AY312890, *nad7* AY330475, *trnL-*
AF306954, *rbcL* U87091, *psbA -*. ***Tetraplodon mnioides***: 18S *F* AY312948, *rps4* AF222902, *rbcL* AY312938, *psbA* AY312923.